



## Electrical isolation and transparency in ion-irradiated p-InGaP/GaAs/InGaAs structures

I. Danilov, L. L. Pataro, M. P. P. de Castro, and N. C. Frateschi

Citation: *Journal of Applied Physics* **88**, 7354 (2000); doi: 10.1063/1.1326462

View online: <http://dx.doi.org/10.1063/1.1326462>

View Table of Contents: <http://scitation.aip.org/content/aip/journal/jap/88/12?ver=pdfcov>

Published by the [AIP Publishing](http://www.aip.org)

---

### Articles you may be interested in

[Annealing characteristics of electrically isolated InGaAsP devices](#)

*Appl. Phys. Lett.* **91**, 062112 (2007); 10.1063/1.2769390

[Thermal stability of ion-irradiated InGaAs with \(sub-\) picosecond carrier lifetime](#)

*Appl. Phys. Lett.* **82**, 856 (2003); 10.1063/1.1543231

[Electrical isolation of InGaP by proton and helium ion irradiation](#)

*J. Appl. Phys.* **92**, 4261 (2002); 10.1063/1.1506200

[Electrical isolation of a silicon  \$\delta\$ -doped layer in GaAs by ion irradiation](#)

*Appl. Phys. Lett.* **75**, 1917 (1999); 10.1063/1.124870

[Electrical isolation of n-type GaAs layers by proton bombardment: Effects of the irradiation temperature](#)

*J. Appl. Phys.* **84**, 4757 (1998); 10.1063/1.368817

---

**Not all AFMs are created equal**  
**Asylum Research Cypher™ AFMs**  
**There's no other AFM like Cypher**

[www.AsylumResearch.com/NoOtherAFMLikeIt](http://www.AsylumResearch.com/NoOtherAFMLikeIt)

  
OXFORD  
INSTRUMENTS  
*The Business of Science®*

The advertisement features a dark blue background with a film strip graphic on the left. The text is in white and orange. The Oxford Instruments logo is in the bottom right corner.

## COMMUNICATIONS

## Electrical isolation and transparency in ion-irradiated *p*-InGaP/GaAs/InGaAs structures

I. Danilov,<sup>a)</sup> L. L. Pataro, M. P. P. de Castro, and N. C. Frateschi<sup>b)</sup>

*Instituto de Física "Gleb Wataghin," Universidade Estadual de Campinas, 13081-970 Campinas, SP, Brazil*

(Received 3 July 2000; accepted for publication 21 September 2000)

He<sup>+</sup>-ion irradiation was applied for electrical isolation of *p*-In<sub>0.49</sub>Ga<sub>0.51</sub>P in InGaP/GaAs/InGaAs structures. Sheet resistance of approximately  $1 \times 10^6 \Omega/\square$  was achieved with doses above  $1 \times 10^{13} \text{ cm}^{-2}$  at 100 keV. Thermal stability of isolation was maintained for annealing temperatures up to 500 °C. Photoluminescence results show that InGaP transparency to InGaAs/GaAs quantum-well emission is closely related to sheet resistance changes in the irradiated structure.

© 2000 American Institute of Physics. [S0021-8979(01)02401-X]

High-power aluminum-free laser structures based on an InGaP/GaAs double heterostructure with a strained InGaAs quantum-well active region are of great interest for erbium-doped fiber amplifiers (EDFA).<sup>1</sup> Output power is limited by mirror catastrophic damage caused mainly by optical absorption at the facets. Ion-implantation-induced quantum-well disordering has been applied to reduce this damage.<sup>2</sup> However, free-carrier absorption in the waveguide and cladding layers at the facets is also important. Aluminum-free structures can also be used for high on-off switching-efficiency three-terminal optical modulators.<sup>3</sup> In these devices, insulating regions are needed along the injection stripes. Wet- and dry-etching techniques<sup>4</sup> provide a rather easy way for electrical isolation. However, in order to attain sufficiently high resistance between electrodes, a deep etching of the InGaP material is required. This leads to discontinuity in the effective index of refraction along the GaAs waveguide and unwanted optical feedback.

Light ion irradiation is an established technique for electrical isolation of III-V semiconductors. It has been shown that ion irradiation of InGaP, similar to GaAs, is capable, in principle, of producing high-resistivity regions in *n*- and *p*-type layers.<sup>5,6</sup> However, basic characteristics of ion-irradiation isolation in InGaP remain unknown (for example, threshold doses of isolation). Again, it is not clear how ion irradiation modifies the optical properties of InGaP, which is treated with the necessary doses to achieve adequate high-resistance value. In this communication, we examine some of the electrical and optical properties of *p*-InGaP material after different stages of He<sup>+</sup>-ion irradiation.

The samples used in this work were grown by chemical-beam epitaxy (CBE) on an *n*-type (100) GaAs substrate. The

epitaxial structure from the substrate is as follows: *n*<sup>+</sup>-GaAs buffer; *n*-InGaP (1.05 μm,  $1 \times 10^{18} \text{ cm}^{-3}$ ); *n*-InGaP (0.15 μm,  $5 \times 10^{17} \text{ cm}^{-3}$ ); undoped GaAs (0.10 μm); undoped In<sub>0.22</sub>Ga<sub>0.78</sub>As quantum well (7 nm) for an emission at  $\lambda = 0.92 \mu\text{m}$  at 77 K; undoped GaAs (0.10 μm); *p*-InGaP (0.10 μm,  $2 \times 10^{17} \text{ cm}^{-3}$ ); *p*-GaAs etch-stop layer (6 nm,  $2 \times 10^{17} \text{ cm}^{-3}$ ); *p*-InGaP (50 nm,  $2 \times 10^{17} \text{ cm}^{-3}$ ); *p*-InGaP (0.91 μm,  $6 \times 10^{17} \text{ cm}^{-3}$ ); *p*-InGaP (0.19 μm,  $1 \times 10^{18} \text{ cm}^{-3}$ ); *p*<sup>+</sup>-GaAs (0.1 μm,  $3 \times 10^{19} \text{ cm}^{-3}$ ), and contact *p*<sup>+</sup>-GaAs layer (0.1 μm,  $> 5 \times 10^{19} \text{ cm}^{-3}$ ). The wafer was cleaved in pieces of 3×6 mm<sup>2</sup>. Ohmic contacts at the edges of the samples were formed by indium strips applied to the *p*<sup>+</sup>-GaAs surface and alloyed at  $\approx 200 \text{ }^\circ\text{C}$  for 2 min. The *p*<sup>+</sup>- and *p*<sup>+</sup>-GaAs contact layers were removed from central parts of the samples by wet etching. Sheet resistance of unirradiated structures was about  $2 \times 10^3 \Omega/\square$ .

The choice of He<sup>+</sup>-ion energy was based on calculations of radiation-defect distributions by the TRIM code.<sup>7</sup> Confining the radiation defects inside the InGaP layer without damage to the InGaAs quantum well is of importance. For 100 keV He<sup>+</sup> ions, the maximum defect density is located at a depth of 0.54 μm, and the radiation damage formation occurs only within the InGaP layer. As He<sup>+</sup>-ion energy augments to 150 keV, the position of maximum defect moves to 0.72 μm. The calculated density of replacement collisions for 150 keV irradiation is equal to  $2 \times 10^2 \text{ cm}^{-1}$  at the InGaAs quantum-well position.

In order to minimize ion channeling effects, ion irradiation was performed with a 15° incidence angle with respect to the sample surface normal. The ion current density was maintained in a range of 5–20 nA/cm<sup>2</sup>. The sheet resistance  $R_s$  values with He<sup>+</sup>-ion dose accumulation were measured after each dose step. Indium contacts protect the contact region from irradiation damages.

Photoluminescence was performed at 77 K with the sample immersed in liquid nitrogen. A 170 mW Ar<sup>+</sup> laser

<sup>a)</sup>Also at: Centro de Componentes Semicondutores-UNICAMP, 13083-970 Campinas, SP, Brazil.

<sup>b)</sup>Author to whom correspondence should be addressed; electronic mail: fratesch@ifi.unicamp.br

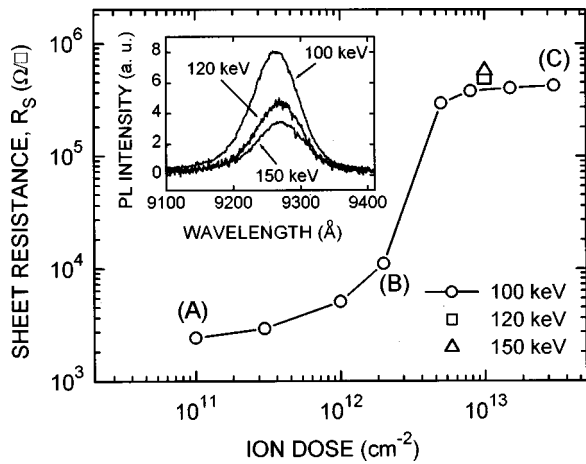


FIG. 1. Sheet resistance  $R_s$  vs  $\text{He}^+$ -ion irradiation dose. The inset shows the photoluminescence spectra after  $1 \times 10^{13} \text{ cm}^{-2}$   $\text{He}^+$  irradiation for different ion energies.

beam,  $\lambda = 0.514 \mu\text{m}$ , and a spot size of approximately  $100 \mu\text{m}$  was used for the optical excitation.

Figure 1 shows the measured sheet resistance versus  $\text{He}^+$ -ion dose accumulation. For doses  $< 1 \times 10^{12} \text{ cm}^{-2}$ , the sheet resistance increases slowly with the dose accumulation. For doses between  $1 \times 10^{12}$  and  $5 \times 10^{12} \text{ cm}^{-2}$  an abrupt increase in  $R_s$  occurs. This buildup of sheet resistance results from a progressive compensation of acceptors by deep-donor defects introduced into the  $p$ -type semiconductor layer during ion irradiation.<sup>8,9</sup> Further dose accumulation has little effect on  $R_s$ , which seems to reach a plateau at  $\approx 4 \times 10^5 \Omega/\square$ .

It is necessary to call attention to the values of the  $R_s$  level in this plateau. This saturation may be an effect of parallel current paths either through a thin unirradiated  $p$ -InGaP material, the GaAs cavity, or the  $n$ -InGaP layer. The first possibility above is evidence by the increase of the plateau  $R_s$  to  $4.9 \times 10^5$  and  $6.6 \times 10^5 \Omega/\square$  after additional  $1 \times 10^{13} \text{ cm}^{-2}$  dose irradiation with  $\text{He}^+$  ions of 120 and 150 keV, respectively. Given the linear character of the current versus voltage dependence of the sheet resistance measurement, transport in the  $n$ -InGaP layer is very unlikely. The typical GaAs cavity layer grown in our CBE system is unintentionally  $p$ -type doped to  $1 \times 10^{15} \text{ cm}^{-3}$ , which has a sheet resistance in the order of  $1.5 \times 10^6 \Omega/\square$ . Therefore, transport through this layer limits our sheet resistance measurements. We can say with reasonable confidence that with an ion-irradiation dose above the threshold  $D_i \approx 8 \times 10^{12} \text{ cm}^{-2}$ , the InGaP sheet resistance is of the order of  $10^6 \Omega/\square$ .

Figure 2 shows the photoluminescence (PL) spectra for a sample with dose accumulations (A), (B), and (C), as indicated in Fig. 1. The inset in Fig. 2 shows the photoluminescence spectrum for the sample prior to irradiation where only InGaP emission at  $\lambda \sim 6000 \text{ \AA}$  is observed. InGaP emission is not observed for any of the irradiated samples. As the irradiation dose increases, a corresponding increase in quantum-well emission PL intensity at  $9260 \text{ \AA}$  is observed.  $\text{He}^+$  irradiation creates nonradiative centers in the InGaP layer. Therefore, quantum-well excitation must, in the best scenario, remain unchanged with ion irradiation. InGaP lay-

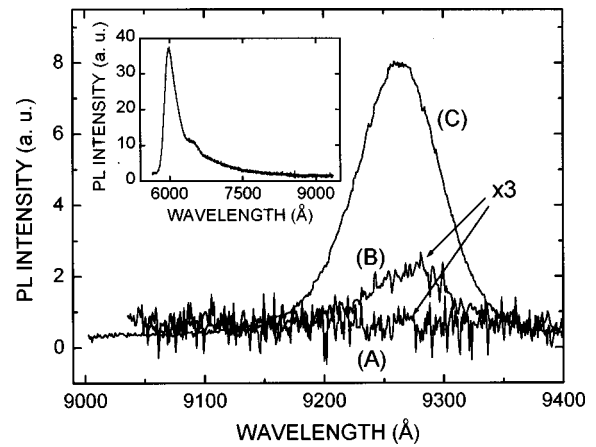


FIG. 2. Photoluminescence spectra of quantum-well emission after  $\text{He}^+$ -ion irradiation with doses (A), (B), and (C), as indicated in Fig. 1. The inset shows the photoluminescence spectrum of an unirradiated structure.

ers will block quantum-well emission mainly by free-carrier absorption and/or photon scattering. A simple Lorentz-Drude model for the doping concentration in the InGaP layer gives a skin depth of 3600 and  $1400 \text{ \AA}$  for the  $1 \times 10^{17}$  and  $1 \times 10^{18} \text{ cm}^{-3}$  hole concentrations, respectively. Therefore, both the increase in  $R_s$  and the increase in InGaP transparency are a consequence of the reduction in free-carrier concentration caused by the  $\text{He}^+$ -ion irradiation. This close relationship between  $R_s$  and transparency indicates that there is no increase in the number of scattering centers in the irradiated layer as is known to occur for high doses of irradiation.<sup>10,11</sup>

At higher  $\text{He}^+$ -ion energies, defects induced by irradiation start to reach the quantum well, reducing its quantum efficiency. The inset in Fig. 1 shows the PL spectra for a sample with a dose of  $1 \times 10^{13} \text{ cm}^{-2}$  for different ion energies. We observe a reduction in quantum-well intensity for energies above 100 keV in agreement with our defect simulations.

The irradiated samples were submitted to thermal annealing steps for 60 s in the temperature range from 100 to

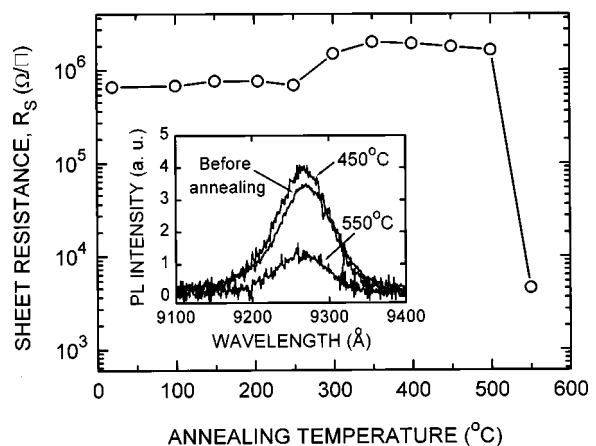


FIG. 3. Sheet resistance  $R_s$  for different annealing temperatures for the sample with an irradiation dose of  $3 \times 10^{13} \text{ cm}^{-2}$ . The inset shows the photoluminescence spectrum for the sample before annealing, and after annealing at 450 and 550 °C.

550 °C in N<sub>2</sub> atmosphere. Figure 3 shows  $R_s$  values versus annealing temperature for the sample with a dose of  $3 \times 10^{13} \text{ cm}^{-2}$ . We found an increase of  $R_s$  by a factor of 3 as the annealing temperature rises to 350–400 °C. Above 500 °C there is a sharp decrease of  $R_s$  to near-unirradiated value. The PL measurements in the inset show a close relationship between  $R_s$  and InGaP transparency for the annealed samples. The maximum PL intensity corresponds to the maximum  $R_s$ , and for temperatures above 500 °C, the quantum-well emission decreases considerably. Since changes in the quantum-well emissions peak position and linewidth are not observed, we believe no quantum-well intermixing is occurring and the change in emission is solely due to a modification in free-carrier absorption in the cladding layer.

Considering the expected small change in index of refraction for the irradiated layer,<sup>12,13</sup> we expect a great reduction in unwanted reflections along the resonant cavity with isolated sections. Finally, with relatively low He<sup>+</sup>-irradiation doses it is possible to create electrically isolated transparent windows in the optical cavity of a laser structure without any damage to the active region. We are currently investigating the effects of ion irradiation on laser facets where the increase in transparency should reduce damages.

In summary, He<sup>+</sup>-ion irradiation was applied for the electrical isolation of *p*-InGaP layers. Resistances of the order of  $1 \times 10^6 \Omega/\square$  were achieved with doses above  $1 \times 10^{13} \text{ cm}^{-2}$  at 100 keV. Thermal stability for annealing temperatures up to 500 °C was achieved. Photoluminescence studies show that InGaP layer transparency to the InGaAs/GaAs quantum-well emissions is closely related to the sheet

resistance, and therefore, there is no evidence of an increase in optical scattering center density with irradiation.

The authors would like to thank J. Bettini for the epitaxial growth of the laser structures and Professor J. W. Swart for the utilization of the Centro de Componentes Semicondutores–State University of Campinas (CCS–UNICAMP) facility. This work was financed by the Fundação de Amparo à Pesquisa do Estado de São Paulo (FAPESP), the Conselho Nacional de Pesquisa e Desenvolvimento (CNPq), and the Coordenação de Aperfeiçoamento de Pessoal de Nível Superior (CAPES).

<sup>1</sup>D. Botez, *Compd. Semicond.* **5**, 24 (1999).

<sup>2</sup>P. G. Piva, S. Charbonneau, R. D. Goldberg, I. V. Mitchel, G. Hillier, and C. Miner, *Appl. Phys. Lett.* **73**, 67 (1998).

<sup>3</sup>N. C. Frateschi, H. Zhao, J. Elliot, S. Siala, M. Govindarajan, R. N. Nottenburg, and P. D. Dapkus, *IEEE Photonics Technol. Lett.* **5**, 273 (1993).

<sup>4</sup>S. J. Pearton, C. R. Abernathy, and F. Ren, *Topics in Growth and Device Processing of III–V Semiconductors* (World Scientific, Singapore, 1996).

<sup>5</sup>S. J. Pearton, J. M. Kuo, F. Ren, A. Katz, and A. P. Perley, *Appl. Phys. Lett.* **59**, 1467 (1991).

<sup>6</sup>H. Strusny, P. Ressel, K. Vogel, and J. Würfl, *Nucl. Instrum. Methods Phys. Res. B* **112**, 298 (1996).

<sup>7</sup>J. F. Ziegler, J. P. Biersack, and U. Littmark, *The Stopping and Range of Ions in Solids* (Pergamon, Oxford, 1985), Vol. 1.

<sup>8</sup>J. P. de Souza, I. Danilov, and H. Boudinov, *Radiat. Eff. Defects Solids* **147**, 109 (1998).

<sup>9</sup>J. P. de Souza, I. Danilov, and H. Boudinov, *Appl. Phys. Lett.* **68**, 535 (1996).

<sup>10</sup>B. Monemar and J. M. Blum, *J. Appl. Phys.* **48**, 1529 (1977).

<sup>11</sup>S. M. Spitzer and J. C. North, *J. Appl. Phys.* **44**, 214 (1973).

<sup>12</sup>B. C. Dobbs, W. J. Andersen, and Y. S. Park, *J. Appl. Phys.* **48**, 5052 (1977).

<sup>13</sup>Q. Kim and Y. S. Park, *Surf. Sci.* **96**, 307 (1980).